Available online at www.sciencedirect.com
SCIENCE DIRECT®
Physics Letters A 317 (2003) 156–164
PHYSICS LETTERS A
www.elsevier.com/locate/pla

Study of the intergrain interaction potential and associated instability of dust-lattice plasma oscillations in the presence of ion flow

I. Kourakis *,1, P.K. Shukla

Institut für Theoretische Physik IV, Fakultät für Physik und Astronomie, Ruhr-Universität Bochum, D-44780 Bochum, Germany

Received 13 June 2003; accepted 14 August 2003

Communicated by F. Porcelli

Abstract

A comprehensive study of the Debye–Hückel repulsive and ion wakefield induced attractive potentials around a dust grain is presented, including ion flow. It is found that the modified interaction potential (especially the attractive wakefield force) can cause instability of linear dust oscillations propagating in a dusty plasma crystal composed of dust grains in a horizontal arrangement suspended in the sheath region near a conducting wall (electrode). The dependence of dust lattice modes on the ion flow is studied, revealing instability of dust lattice modes for certain values of the ion flow speed.

PACS: 52.27.Lw; 52.35.Fp; 52.25.Vy

About a decade ago, several groups [1–4] observed the formation of dusty plasma crystals in low-temperature laboratory discharges. Dusty plasma (DP) crystals/quasi-lattices are typically formed in the vicinity of a conducting wall (electrode) in gas discharge experiments, and they are suspended at a levitation height where the sheath electric and gravity forces balance. Physically, the dust grain crystallization occurs owing to some attractive forces [5] which dominate over the Debye–Hückel repulsive force. Nambu et al. [6] were the first to introduce a novel attractive force between two equal sign dust grains due to the wakefield and ion focusing involving dust ion-acoustic and dust acoustic waves in dusty plasmas without and with ion flow [7–9]. The wakefield idea has been experimentally verified in a vertical chain in which a lower dust particle is attracted towards the upper particle in a plasma with ion flow [10–12]. A recent theoretical study [13] reexamines the modification of the Debye–Hückel repulsive and wakefield attractive potentials in an unmagnetized dusty plasma including ion flow in the sheath region.

The oscillations of dust particles in dusty plasma crystals admit longitudinal [14–17] and transverse [16–19] dust lattice waves. In the latter, the restor-

* Corresponding author.
E-mail addresses: ioannis@tp4.rub.de (I. Kourakis), ps@tp4.rub.de (P.K. Shukla).
[1] On leave from: ULB, Université Libre de Bruxelles, Faculté des Sciences Apliquées, C.P. 165/81 Physique Générale, Avenue F.D. Roosevelt 49, B-1050 Brussels, Belgium.

0375-9601/$ – see front matter
doi:10.1016/j.physleta.2003.08.020

ing force is associated with the Debye–Hückel repulsive interaction between two neighboring dust grains, while the dust mass provides the inertia to maintain the dust lattice oscillations. Both longitudinal and transverse dust lattice oscillations have been observed experimentally [20–22].

In this Letter, we present a comprehensive investigation of intergrain potential energy in the presence of ion flow in plasmas. Specifically, we exploit the results of Ref. [13] to provide detailed information regarding the role of ion flow on short range Debye–Hückel and long range attractive potentials around dust grains that are levitated at the same height above a negative electrode. It is shown that both short and long range potentials are modified by the ion flow. We then carry out a study of the stability of dust oscillations in a horizontal arrangement of a dust chain, including the repulsive and attractive forces. It is found that dust lattice modes may become unstable due to ion flow towards the electrode.

Let us consider dust lattice oscillations in a plasma whose constituents are electrons, streaming ions, and an ensemble of negatively charged dust grains. The *longitudinal* motion of charged dust grains (the mass M and charge Q, both assumed constant for simplicity) in a DP crystal (lattice constant r_0) obeys an equation of the form

$$M\left(\frac{d^2x_n}{dt^2}+\nu\frac{dx_n}{dt}\right)=-\sum_n\frac{U_{nm}(r_{nm})}{\partial r}\equiv QE(x_n), \tag{1}$$

where $U_{nm}(r_{nm})\equiv Q\phi(x)$ is a binary interaction potential function related to the electrostatic potential $\phi(x)$ around the mth grain, and $E(x)=-\partial\phi(x)/\partial x$ is the electric field, $r_{nm}=x_n-x_m$ is the distance between the nth and mth grains. Finally, ν denotes the damping rate due to dust–grain collisions with neutrals. A one-dimensional (1d) DP layer is considered here, but the generalization to a two-dimensional (2d) grid is straightforward. Retaining only first neighbor interactions and considering small (linear) longitudinal displacements $\delta x_n=x_n-x_n^{(0)}$ around the equilibrium position $x_n^{(0)}$ of the nth grain, one obtains

$$\frac{d^2\delta x_n}{dt^2}+\nu\frac{\delta x_n}{dt}=\omega_{0,\mathrm{L}}^2(\delta x_{n-1}+\delta x_{n+1}-2\delta x_n). \tag{2}$$

The longitudinal dust lattice (LDL) oscillation 'eigenfrequency' $\omega_{0,\mathrm{L}}$ is given by

$$\omega_{0,\mathrm{L}}^2=\frac{Q}{M}\frac{\partial^2\phi(r)}{\partial r^2}\bigg|_{r=r_0}. \tag{3}$$

For instance, $\phi(r)$ is often assumed to be the Debye–Hückel potential

$$\phi^{(\mathrm{D})}(r)=\frac{Q}{r}\exp(-k_\mathrm{D}r), \tag{4}$$

where $k_\mathrm{D}=\lambda_\mathrm{D}^{-1}$ and λ_D is the Debye radius. In a dusty plasma, a dust grain is typically shielded by ions when electrons and ions are in thermodynamical equilibrium. However, in a plasma with flowing ions, the Debye shielding is due to electrons, and hence $\lambda_\mathrm{D}=\lambda_\mathrm{De}$. The frequency $\omega_{0,\mathrm{L}}$ of the dust longitudinal mode then turns out to be [5,14–16]

$$\omega_{0,\mathrm{L}}^{(\mathrm{D})2}=\frac{2Q^2}{Mr_0^3}\left(1+\frac{r_0}{\lambda_\mathrm{D}}+\frac{r_0^2}{2\lambda_\mathrm{D}^2}\right)\exp(-k_\mathrm{D}r_0).$$

Assuming displacements of the form $\delta x_n=\delta x_n^{(0)}\times\exp[i(nkr_0-\omega t)]$, the longitudinal dust lattice wave (LDLW) equation (2) yields the linear dispersion relation

$$\omega(\omega+i\nu)=4\omega_{0,\mathrm{L}}^2\sin^2\left(\frac{kr_0}{2}\right), \tag{5}$$

which reduces to

$$\omega(\omega+i\nu)\approx\omega_{0,\mathrm{L}}^2r_0^2k^2\equiv c_\mathrm{L}^2k^2 \tag{6}$$

in the continuum (long-wavelength) limit, i.e., for $\lambda\gg r_0$. We see that the stability of the LDLW is ensured only if the right-hand side is positive, i.e., if (and only if) $\omega_{0,\mathrm{L}}$ is real (viz. $\omega_{0,\mathrm{L}}^2>0$); otherwise, the slightest displacement from equilibrium may result in an unstable mode. Therefore, stability basically depends on the interaction potential $\phi(r)$ via $\omega_{0,\mathrm{L}}$; see Eq. (3) above.

For comparison, the *transverse* ($\|z$) displacement (assumed to be decoupled from the longitudinal one) of dust grains (assumed at fixed sites at $x_n=nr_0$) in the same DP lattice obeys the equation

$$M\left(\frac{d^2z_n}{dt^2}+\nu\frac{dz_n}{dt}\right)=-\sum_n\frac{U_{nm}(r_{nm})}{\partial r}\bigg|_{r=r_0}+F_\mathrm{el}-Mg, \tag{7}$$

where the electric force $F_{\rm el}(z)$ is related to the (externally imposed) sheath potential. Once again, by considering small (linear) longitudinal displacements $\delta z_n = z_n - z_0$ around the (equilibrium) levitation height z_0 (where $F_{\rm el}|_{z_0} - Mg = 0$), and keeping first neighbor interactions only, one obtains the transverse dust lattice wave (TDLW) equation [5]

$$\frac{d^2\delta z_n}{dt^2} = \omega_{0,\rm T}^2(2\delta z_n - \delta z_{n-1} - \delta z_{n+1}) + F_{\rm el} - Mg, \tag{8}$$

where $\omega_{0,\rm T}$ is the transverse oscillation eigenfrequency determined from

$$\omega_{0,\rm T}^2 = -\frac{Q}{Mr_0}\frac{\partial\phi(r)}{\partial r}\bigg|_{r=r_0}, \tag{9}$$

which is equal, for instance, to

$$\omega_{0,\rm T}^{(\rm D)2} = \frac{Q^2}{Mr_0^3}\left(1 + \frac{r_0}{\lambda_{\rm D}}\right)\exp(-k_{\rm D}r_0)$$

in the Debye–Hückel case. The TDLW optic-mode-like dispersion relation reads

$$\omega(\omega + i\nu) = \omega_{\rm g}^2 - 4\omega_{0,\rm T}^2\sin^2\left(\frac{kr_0}{2}\right), \tag{10}$$

where the gap frequency $\omega_{\rm g}$ is related to $F_{\rm el}$. For $kr_0 \ll 1$, we have

$$\omega(\omega + i\nu) \approx \omega_{\rm g}^2 - \omega_{0,\rm T}^2 r_0^2 k^2 \equiv \omega_{\rm g}^2 - c_{\rm T}^2 k^2. \tag{11}$$

As in the LDLW case above, the stability profile depends on the interaction potential via $\omega_{0,\rm T}$; see Eq. (9). In particular, stability is ensured ($\forall k$) only if $\omega_{0,\rm T}^2/\omega_{\rm g}^2 < 1/4$.

In a more sophisticated description, one should take into account the wake potential generated by ion flow towards the electrode [7,13]. It has been recently shown from first physical principles [13] that the electrostatic interaction potential $\phi(r) = Qk_{\rm D}W(r)$ around a charged dust grain in the vicinity of a conducting wall penetrated by in-flowing ions may strongly deviate from the simple Debye–Hückel picture. Employing an appropriate integral transform formalism (with respect to the z-coordinate), i.e., defining the Green function

$$G_{\mathbf{k}_\perp}(z_0) = \int d\mathbf{r}_\perp\, W(\mathbf{r}_\perp; z_0)\exp(-i\mathbf{k}_\perp\mathbf{r}_\perp), \tag{12}$$

elaborating its analytic form and then inverting back to real space, viz.

$$W(\mathbf{r}_\perp; z_0) = \frac{1}{(2\pi)^\delta}\int d^\delta\mathbf{k}_\perp\, G_{\mathbf{k}_\perp}(z_0)\exp(i\mathbf{k}_\perp\mathbf{r}_\perp), \tag{13}$$

($\delta = 1, 2$)[2] the (normalized) potential $W(r; z_0)$ expressing the interaction between horizontally ($\perp z$) arranged dust grains (charge Q, mass M), situated at a distance $r \equiv \rho\lambda_{\rm D}$, levitated at the same height $z = z_0 \equiv a\lambda_{\rm D}$ above a negative conducting wall (located at $z = 0$) and exposed to ion flow at velocity u, was found in Ref. [13] to be

$$W(\rho) = 2\int_0^\infty dq_\perp\, q_\perp J_0(q_\perp\rho)g(k), \tag{14}$$

where $g(k) = (k_{\rm D}/4\pi)G_{\mathbf{k}_\perp}(z_0)$ is the (dimensionless) function, given by

$$g(k) = \frac{e^{-\kappa a}}{\kappa^2 + q^2}\big[\kappa\sinh(\kappa a) + q\sin(qa)\big] \tag{15}$$

and $J_0(x)$ is a Bessel function of the first kind.[3] The quantities q and κ, related to the poles of the dielectric function, are defined as

$$\begin{aligned} q^2 &= \frac{1}{2}\Big[\sqrt{\big(q_\perp^2 + 1 - M^{-2}\big)^2 + 4M^{-2}q_\perp^2} \\ &\qquad - q_\perp^2 + M^{-2} - 1\Big], \\ \kappa^2 &= \frac{1}{2}\Big[\sqrt{\big(q_\perp^2 + 1 - M^{-2}\big)^2 + 4M^{-2}q_\perp^2} \\ &\qquad + q_\perp^2 - M^{-2} + 1\Big], \end{aligned} \tag{16}$$

where M ($= uk_{\rm D}/\omega_{\rm i}$) is the Mach number and $\omega_{\rm i}$ is the ion plasma frequency. The intergrain distance r, levitation height z_0 and wavenumber k enter the preceding formulae through the re-scaled variables $\rho = r/\lambda_{\rm D}$, $a = z_0/\lambda_{\rm D}$ and $q_\perp = k\lambda_{\rm D}$, respectively. Notice, however, that the latter is integrated out in (14), so that $W = W(r; z_0) = W(\rho; a)$.

Note that the first term in the right-hand side of (15) is related to the Debye–Hückel potential

[2] $\delta = 1$ (2) for a one- (two-)dimensional lattice. Expression (14) has been derived for $\delta = 2$; for $\delta = 1$, set $\int_0^\infty dq_\perp\, q_\perp J_0(q_\perp\rho) \to \frac{1}{2\pi}\int_{-\infty}^\infty dq_\perp\cos(q_\perp\rho)$.

[3] See footnote 2.

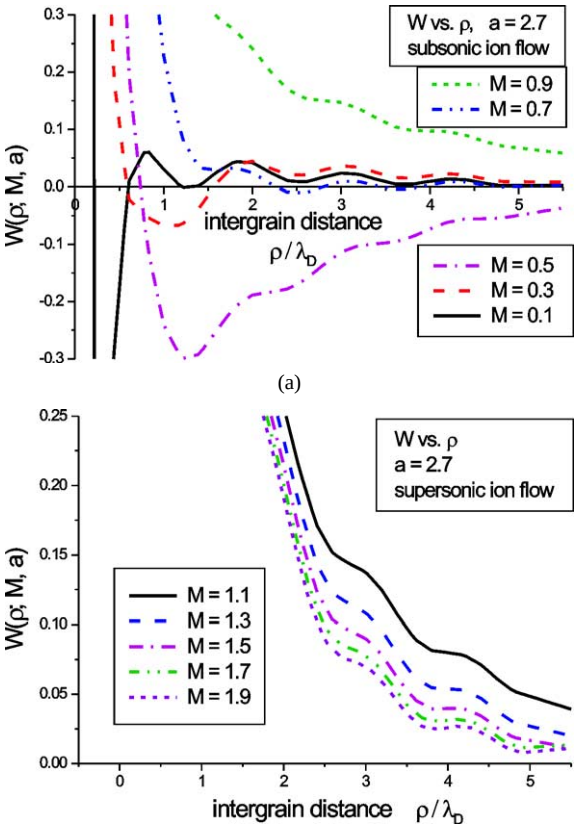

Fig. 1. The normalized interaction potential W is depicted against the (normalized) intergrain distance $k_D r$, for $a = 2.7$. (a) Subsonic ion flow ($M < 1$). (b) Supersonic ion flow ($M > 1$).

(distorted by the ion flow), while the second term accounts for the wake potential generated downstream by grains. Indeed, considering the limit of vanishing ion velocity ($u_i \to 0$)[4] and infinite electrode-to-grain distance ($a \to \infty$), the well-known Fourier transform of the Debye potential is recovered, i.e., $g(k) \to 1/(1+q_\perp^2)^{1/2} \equiv k_D/(k_D^2+k^2)^{1/2}$.

[4] Canceling the ion flow consists in omitting its contribution to the dielectric function $\epsilon(\mathbf{k})$, i.e., the second term in the right-hand side of expression (2) in Ref. [13], thus switching off the ions (but still keeping the distinction between the z-direction and the x–y plane, introduced therein). The zeroes of $\epsilon(\mathbf{k})$ then become $k \to \pm i k_D$, and the poles in the k_z-integration—follow the passing from (3) to (5) in Ref. [13]—are expressed as $k_\parallel \to 0$ and $k_\parallel \to \pm i(k_D^2+k_\perp^2)^{1/2}$, i.e., $q \to 0$ and $\kappa \to \pm(1+q_\perp^2)^{1/2}$. Technically (and rather against intuition) this amounts to considering the limit $M^{-1} \to 0$ in (16) and related formulae in the text.

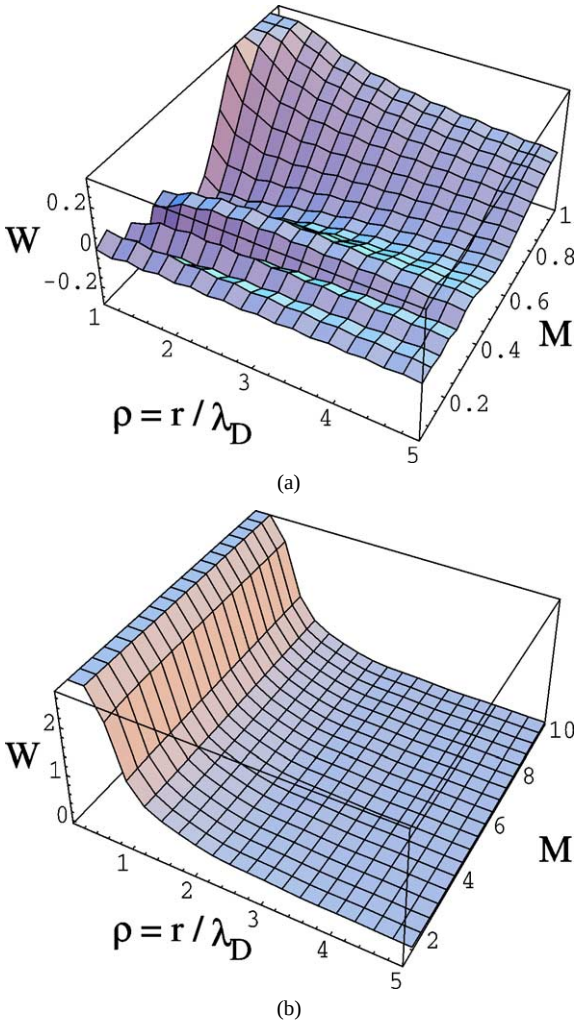

Fig. 2. The interaction potential W is depicted against the (normalized) intergrain distance $\rho = k_D r$ and the Mach number M, for $a = 2.7$. (a) Subsonic ion flow ($0 < M < 1$). (b) Supersonic ion flow ($1 < M < 10$). We see that the character (attractive/repulsive) of the potential w at a given distance $\rho = k_D r$ may depend on the subsonic ion flow.

A preliminary analysis of the preceding formulae (14)–(16) in the asymptotic (long range, i.e., for $\rho \to \infty$) limit was carried out in Ref. [13] where the dependence of the interaction potential on M and a was discussed; relying on a simple two-dimensional dust gas (grid) model, it was qualitatively shown that dust grain oscillations subject to a subsonic ion flow may become unstable for certain (combined) values of M and a. It was shown therein that the frequency ω of

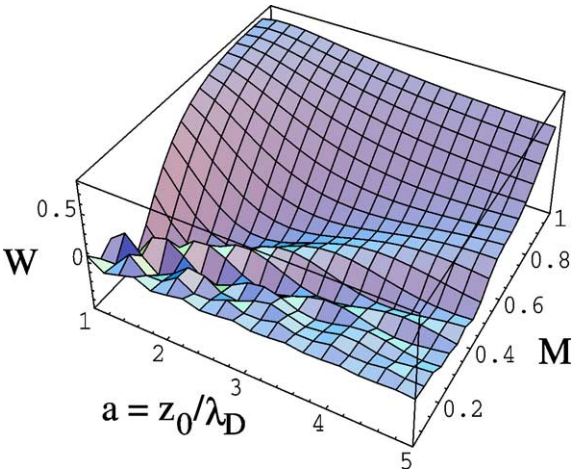

(a)

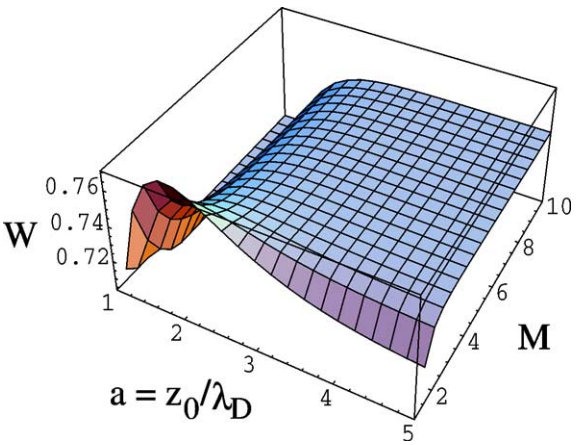

(b)

Fig. 3. The interaction potential W is depicted against the (normalized) levitation height a ($1 < a < 5$ here) and the Mach number M, for an intergrain distance value of $\rho = k_{\mathrm{D}} r = 1$. (a) Subsonic ion flow ($0 < M < 1$). (b) Supersonic ion flow ($1 < M < 10$). The character (attractive/repulsive) of the potential w at a given height may depend on the (subsonic) ion velocity, and vice versa.

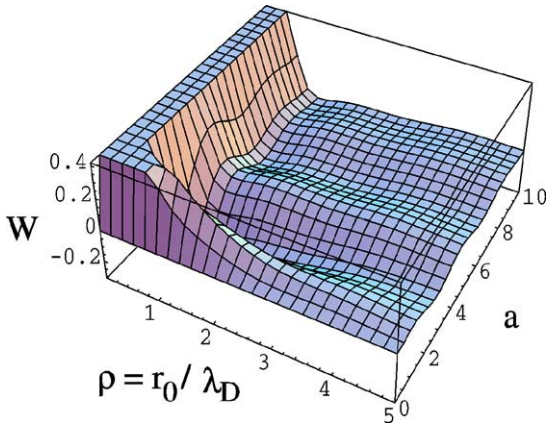

(a)

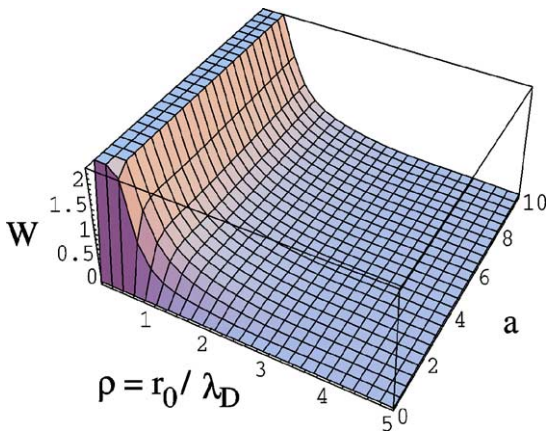

(b)

Fig. 4. The potential W is represented against the (normalized) levitation height a ($0 < a < 10$) and the intergrain distance $\rho = k_{\mathrm{D}} r$ ($0 < \rho < 5$) for a fixed Mach number M, equal to (a) $M = 0.5$, (b) $M = 1.5$. Notice that a given distance may correspond to stable or unstable oscillations, depending on the levitation height.

oscillations in the grid is given by the expression

$$\omega^2 \approx \frac{Q^2}{M\lambda_{\mathrm{D}}^3} g(k) k^2 \tag{17}$$

(up to a factor $1/\pi$); see Eq. (19) in [13]. Therefore, the sign of ω^2 may be investigated by a numerical analysis of the (sign of the) right-hand side in (17).

In a similar manner, one may derive the corresponding characteristic frequency of longitudinal oscillations $\omega_{0,\mathrm{L}}^2$ from the equation of motion (2), given by (3). Combining with (13) (remember that $\nabla^n = (i\mathbf{k})^n$ in Fourier space), we see that $\omega_{0,\mathrm{L}}^2$ entering the dispersion relations (5) and (6), is related to the potential (Fourier) transform $G_{\mathbf{k}_\perp} = (4\pi/k_{\mathrm{D}}) g(k)$ via the expression

$$\omega_{0,\mathrm{L}}^2 = -\frac{Q^2}{M} \frac{1}{(2\pi)^\delta} \int d^\delta \mathbf{k}_\perp k^2 G_{\mathbf{k}_\perp}(z_0) \exp(i\mathbf{k}_\perp \mathbf{r}_0), \tag{18}$$

i.e.,

$$\omega_{0,\mathrm{L}}^2 = -\frac{2Q^2 k_{\mathrm{D}}^3}{M} \int_{-\infty}^{\infty} dq_\perp q_\perp^2 g(q_\perp) \cos(q_\perp \rho_0) \tag{19}$$

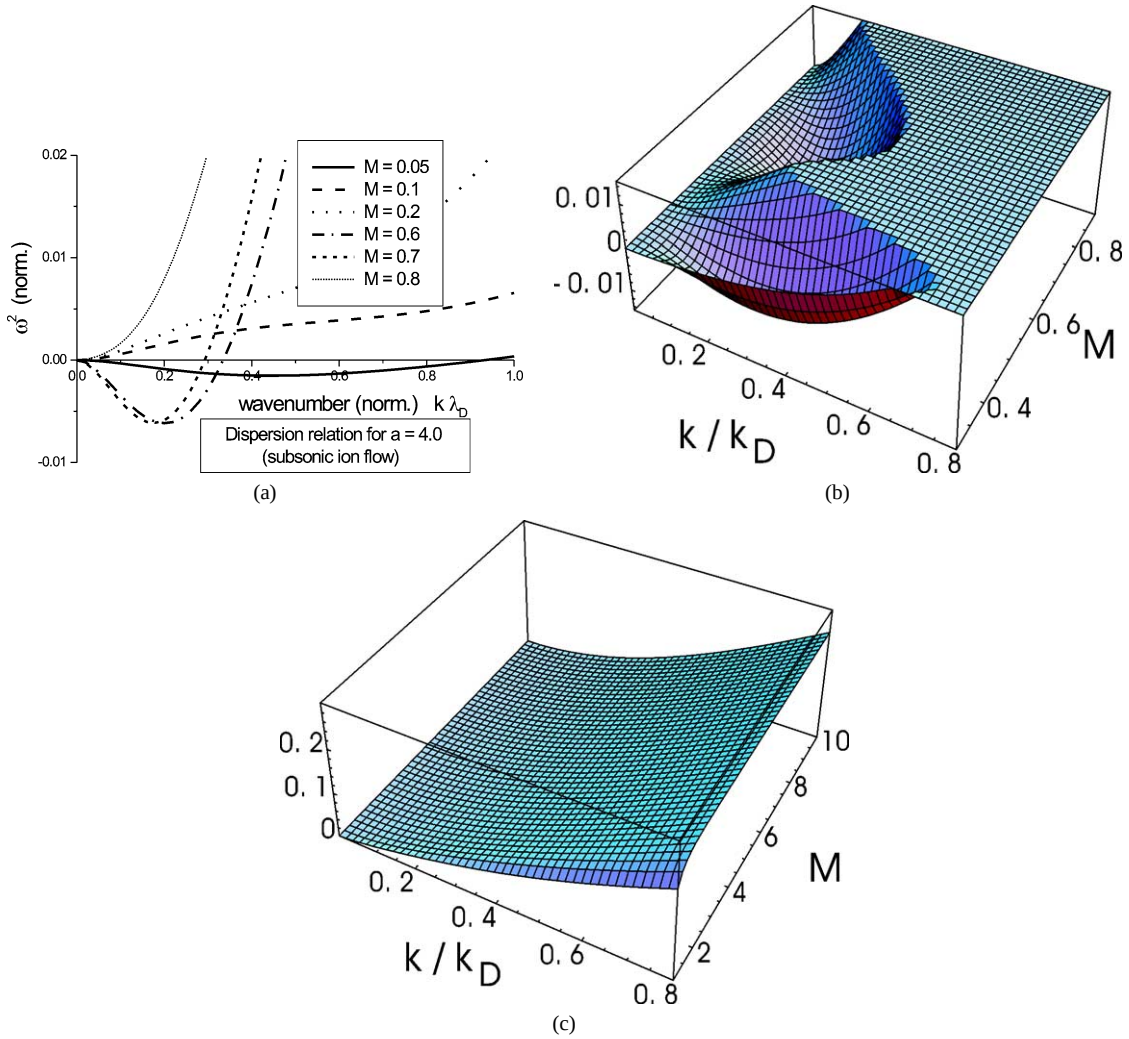

Fig. 5. (a) The dust grid dispersion curve, i.e., the oscillation frequency squared ω^2, as given by (15) and (17), is represented vs. the wavenumber k (normalized by k_{D}). (b) ω^2 is depicted against the wavenumber k and the Mach number M ($0 < M < 1$: subsonic case). (c) As in (b), for the supersonic case ($M > 1$). The levitation height was chosen equal to $a = 2.7$. Stable ($\omega^2 > 0$) and unstable ($\omega^2 < 0$) regions are clearly distinguished in (a) and (b). Notice that two distinct unstable regions appear—see the dips in (b)—as the ion velocity increases. The supersonic case is globally stable.

for a one-dimensional lattice ($\delta = 1$). Notice that this final expression for the characteristic lattice oscillation frequency $\omega_{0,\mathrm{L}}$ depends on both the levitation height $a = k_{\mathrm{D}} z_0$ (via the function g, defined in (15)) and the lattice constant $\rho_0 = r_0/\lambda_{\mathrm{D}}$. In order to investigate the sign of $\omega_{0,\mathrm{L}}^2$, which reflects, as previously stated, the stability of the lattice oscillations, one is left with the task of evaluating the right-hand side in (19) numerically. The remaining part of this Letter is devoted to a rigorous and exact numerical study of the behaviour of the interaction potential, as given by the above expressions, as well as an investigation of the stability of longitudinal modes in the preceding model.

The behaviour of the potential W against intergrain distance ρ, at a fixed (normalized) height a, is depicted in Fig. 1. In the subsonic regime ($M < 1$), we encounter the appearance of attractive interaction regions, as qualitatively predicted in Ref. [13], which are then smoothed out as M takes higher values, and disappears completely in the supersonic regime ($M > 1$).

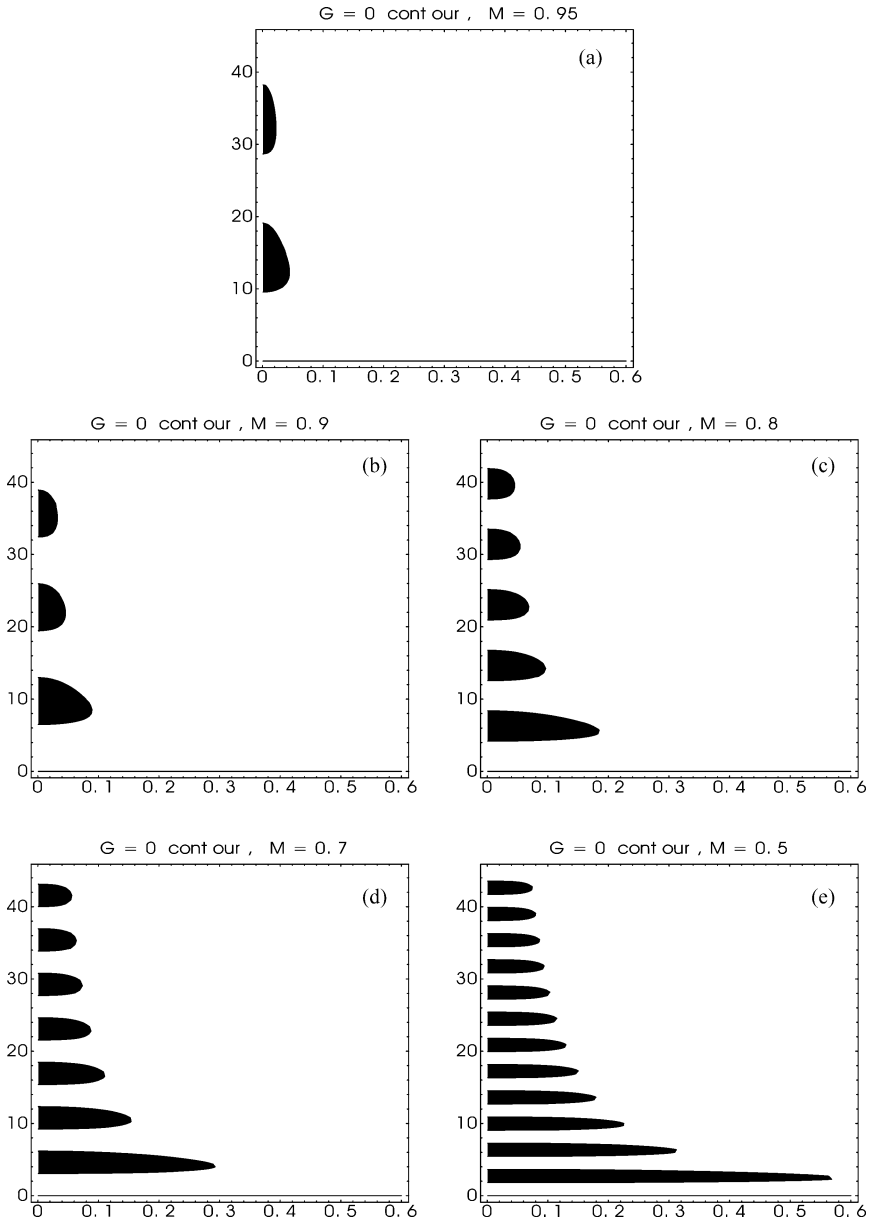

Fig. 6. Dust grid (in)stability contours (cf. (15), (17)): $\omega^2 = 0$ boundary curves are depicted against the (normalized) wavenumber k/k_{D} and the levitation height a, for M equal to 0.95, 0.9, 0.8, 0.7, 0.5 (subsonic ion flow), respectively, in (a) to (e). As we move far from the electrode (a takes higher values), instability is smoothed out. We observe that instability appears as the ion flow is gradually slowed down. The corresponding contour plot in the supersonic case $M > 1$ (not depicted) is filled in white colour (stability); cf. Fig. 3 in Ref. [13].

In general, the stability of dust lattice oscillations, as well as the character of the interaction potential (attractive/repulsive) depends on the physical parameters involved, namely: (i) the intergrain equilibrium distance ρ, (ii) the levitation height a and (iii) the ion flow (via the Mach number M) in a rather complex manner. Figs. 2–4 represent a set of three-dimensional plots of the interaction potential $W(r)$ as a function of two of these parameters, keeping the third one fixed. For instance, keeping the levitation height fixed (see

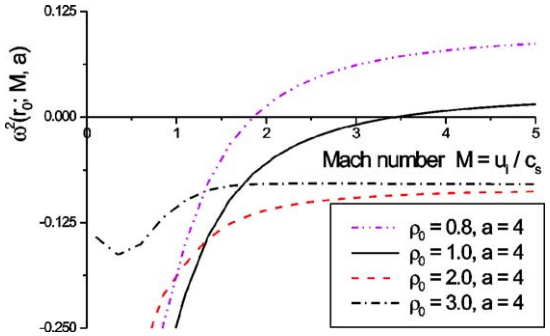

Fig. 7. The characteristic (square) lattice frequency $\omega_{0,\mathrm{L}}^2$, given by (19), is depicted against the Mach number M for fixed (levitation height) a and different values of the (normalized) lattice constant $\rho_0 = r_0/\lambda_\mathrm{D}$.

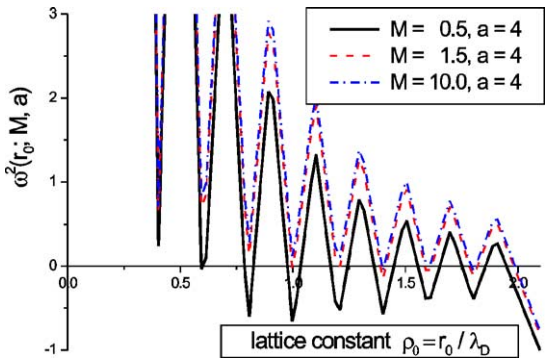

Fig. 8. The characteristic (square) lattice frequency $\omega_{0,\mathrm{L}}^2$, given by (19), is depicted against the (normalized) lattice constant $\rho_0 = r_0/\lambda_\mathrm{D}$ for fixed (levitation height) a and different values of the Mach number M.

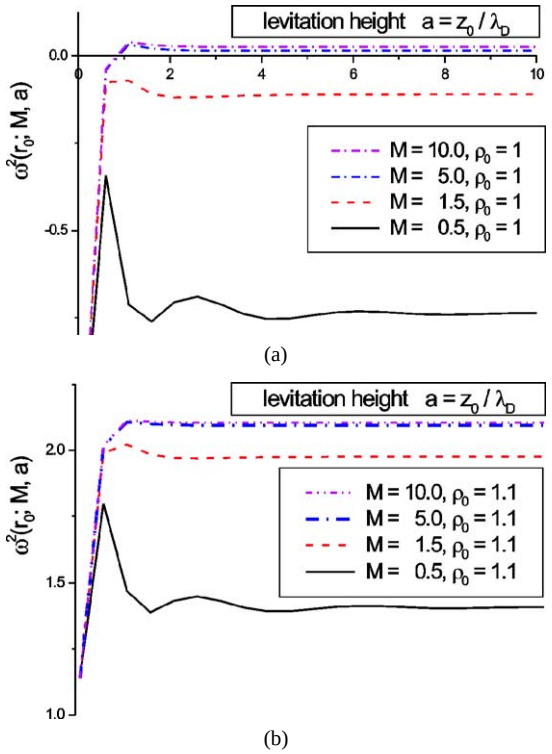

Fig. 9. $\omega_{0,\mathrm{L}}^2$ is depicted against the (normalized) levitation height a for different values of the Mach number M and lattice constant: (a) $\rho_0 = 1.0$; (b) $\rho_0 = 1.1$. We see that the latter is always stable, while the former is only stable at specific height values a.

Fig. 2), we notice that the form of the potential $W(r)$ may strongly differ between one value of the Mach number M and another. In a similar manner, the numerical value of the potential form at a given value of the intergrain distance ρ may strongly depend on the levitation height a in combination with the surrounding ion flow; see Fig. 3. Finally, for a given value of the Mach number M, the form of the potential $w(r)$ vs. r may be qualitatively different at different levitation heights a; see Fig. 4. Nevertheless, as intuitively expected, for high values of a, i.e., far from the wall, the electrode effect is smoothed out, so what remains is the repulsive Debye potential, slightly distorted by the ion flow. It should be stressed that all the above results are valid in the subsonic case ($M < 1$). Supersonic ion flow seems to have little effect on the qualitative form of the interaction potential, which remains repulsive—see, e.g., Fig. 3(b)—ensuring oscillatory stability (as we shall also see below).

In the case of the dust-grid introduced in Ref. [13], a negative value of ω^2, as given by (15) and (17), implying a purely growing mode, is indeed allowed to occur for certain value combinations of the physical parameters involved; see Figs. 5 and 6. In a general manner, we see that oscillations for a given value of distance ρ and height a may be stable for certain values of M and become unstable as M varies. For $M < 1$, a similar effect is present with respect to a, i.e., oscillations for a given value of ρ and M may be stable for certain values of height a and become unstable as the latter varies, i.e., essentially changing the sheath electric field (related to the levitation height viz. $QE|_{z=z_0} = Mg$); see the stability contour plots in Fig. 6.

A similar analysis may be carried out with respect to the chain's stability profile, in terms of the sign of ω^2, as given by (19). As intuitively expected, the stability of the chain for a given value of ρ depends on the velocity u_i of the ion flow, so that an increase in u_i may result in unstable oscillations and melting of the chain. Inversely, stability for given u_i may be ensured for a certain value of ρ and excluded for another; cf. Figs. 7 and 8 (the latter is reminiscent of the oscillatory space variation of the wake potentials pointed out in previous works). Notice that, in general, stable configurations correspond to lattice constants of the order of a Debye length λ_D, in agreement with known experimental results. On the other hand, the dependence on the levitation height a (for given u_i, ρ) does not appear to be so dramatic: stable configurations remain so while varying a; nevertheless, different values of ρ—yet possibly close ones—may present a completely different stability profile; cf. Fig. 9(a), (b). These remarks seem to suggest that melting may occur when modifying the ion flow and/or when strong intergrain distance variations occur (possibly related to wide amplitude longitudinal oscillations due to nonlinear effects), yet rather not so if the equilibrium position (related to the linear term in the sheath field) is modified. Interestingly, all the above remarks remain valid in both sub- ($M < 1$) and supersonic ($M > 1$) ion flow cases (in contrast with the Ignatov grid model [13], where stability was prescribed for $M > 1$).

In conclusion, we have presented a complete study of the interaction potential between two negatively charged dust grains in an unmagnetized plasma with ion flow. It is found that both Debye–Hückel repulsive and ion wake attractive potentials are significantly modified by the ion flow. The attractive ion wake force can produce a phase shift between the dust charge density and the dust position in dust grain arrangements suspended in the vicinity of a conducting electrode. Consequently, the dust lattice oscillations become unstable. The instability regimes are sensitive to the ion flow speed. The present results may help to understand the melting of dust crystals in the sheath where ions are streaming against charged dust grains which form a dust lattice.

In closing, we mention that our investigation of the longitudinal dust lattice waves in the presence of modified Debye–Hückel and ion wake potentials follows Ivlev and Morfill [23] and considers only the nearest neighbor dust particle interactions. The latter is valid as long as $r_d \ll a \ll \lambda_D$, where r_d is the dust radius, a is the intergrain separation distance, and λ_D is the effective Debye radius of an unmagnetized dusty plasma. On the other hand, when $a \sim \lambda_D$, the approximation of nearest neighbor dust grain interaction has to be relaxed in order to obtain the modified spectrum [15,17] of longitudinal dust lattice waves in an infinite chain of charged dust; however, this investigation is beyond the scope of the present Letter.

Acknowledgements

This work was partially supported by the European Commission (Brussels) through the Human Potential Research and Training Network via the project entitled: Complex Plasmas: The Science of Laboratory Colloidal Plasmas and Mesospheric Charged Aerosols (Contract No. HPRN-CT-2000-00140).

References

[1] J.H. Chu, et al., Phys. Rev. Lett. 72 (1994) 4009.
[2] H. Thomas, et al., Phys. Rev. Lett. 73 (1994) 652.
[3] A. Melzer, et al., Phys. Lett. A 191 (1994) 301.
[4] Y. Hayashi, K. Tachibana, Jpn. J. Appl. Phys. 33 (1994) L84.
[5] P.K. Shukla, A.A. Mamun, Introduction to Dusty Plasma Physics, Institute of Physics, Bristol, 2002.
[6] M. Nambu, et al., Phys. Lett. A 203 (1995) 40.
[7] P.K. Shukla, N.N. Rao, Phys. Plasmas 3 (1996) 1770.
[8] O. Ishihara, et al., Phys. Plasmas 4 (1997) 69.
[9] G. Lapenta, Phys. Rev. E 66 (2002) 026409.
[10] K. Takahashi, et al., Phys. Rev. E 58 (1998) 7805.
[11] A. Melzer, et al., Phys. Rev. Lett. 83 (1999) 3194.
[12] G.E. Morfill, et al., in: P.K. Shukla, et al. (Eds.), Advances in Dusty Plasma Physics, World Scientific, Singapore, 1997, p. 99;
G.E. Morfill, et al., Phys. Rev. Lett. 83 (1999) 1598.
[13] A.M. Ignatov, Plasma Phys. Rep. 29 (2003) 296.
[14] F. Melandsø, Phys. Plasmas 3 (1996) 3890.
[15] B. Farokhi, et al., Phys. Lett. A 264 (1999) 318;
B. Farokhi, et al., Phys. Plasmas 7 (2000) 814.
[16] O. Ishihara, et al., Phys. Scripta T 75 (1998) 79.
[17] D. Tskhakaya, P.K. Shukla, Phys. Lett. A 286 (2001) 277.
[18] S.V. Vladimirov, et al., Phys. Rev. E 56 (1997) R74.
[19] X. Wang, et al., Phys. Rev. Lett. 86 (2001) 2569.
[20] A. Homann, et al., Phys. Rev. E 56 (1997) 7138.
[21] A.V. Ivlev, et al., Phys. Rev. Lett. 85 (2000) 4060.
[22] T. Misawa, et al., Phys. Rev. Lett. 86 (2001) 1219.
[23] A.V. Ivlev, G. Morfill, Phys. Rev. E 63 (2001) 016409.